Effect of Equal Channel Angular Extrusion on the Microstructure and Superplasticity of an Al-Li Alloy

H.G. Salem and J.S. Lyons

(Submitted 30 July 2001; in revised form 2 April 2002)

This research investigates the use of equal channel angular extrusion (ECAE) processing to produce a superplastic form of the aluminum alloy 2098. The starting material was a hot-rolled and precipitation-hardened plate with elongated grains of width 67-92 μm, and a composition in weight percent of 2.2% Li, 1.3% Cu, 0.73% Mg, 0.05% Zr, balance Al. Microstructural evolution was investigated with optical and transmission electron microscopy (TEM) and microhardness measurements after each step of a multipass ECAE process. ECAE produced a submicron grain structure with an average size of about 0.5 μm. The sub-grain microstructure size was a function of the magnitude of the input strain and the extrusion temperature. Misorientation angles of the developed submicron structure increase with increasing number of passes at warm working temperatures. Superplastic behavior of the ECAE-processed alloy was achieved. However, the low zirconium content of the 2098 alloy resulted in grain growth of the refined structure at the superplastic processing temperatures, placing a lower limit on the deformation rates that can be used.

Keywords aluminum alloy 2098, equal channel angular extrusion, submicron grain structure, superplasticity

1. Introduction

Most superplastic alloys are produced by conventional processing techniques such as rolling and extrusion. These materials have grain sizes in the range of 2-10 μm and are usually superplastically formed at elevated temperatures of 0.8 T_m, and low strain rates of 10^{-4} s^{-1}. Other superplastic alloys, manufactured from powder metallurgy or mechanical alloying, have a finer grain structure and can be superplastically formed at relatively lower temperatures and higher strain rates.[1-3] However, powder metallurgy and mechanical alloying are relatively more expensive than ingot metallurgy. It would therefore be cost effective to produce a material with a submicron grain structure, which is capable of enhancing the superplastic behavior at lower temperatures and/or higher deformation rates, using bulk processing techniques.

Equal channel angular extrusion (ECAE) is a material-processing technique through which a cast ingot is subjected to intense plastic straining, which produces submicron grain structure without residual porosity. ECAE processing involves the intense deformation of the material through two channels of equal cross-section intersecting at an angle ϕ that varies between 60-120°.[4, 5] Figure 1 shows a schematic representation of the ECAE process. Since the two sections of the channels within the die are equal in cross section, there is no change in the billet dimensions during processing. This facilitates repetitive extrusion through the ECAE channels. The intense plastic straining of the billets takes place at the intersection line between the two channels, where the material is subject to simple shear strain, the magnitude of which depends on the angle ϕ. One important characteristic of ECAE is its ability to fragment the bulk material's structure by simple shear into a very fine grain size (0.2 μm) one order of magnitude less than that produced by any conventional processing method.[6, 7] In addition, the ECAE process has proven that it is capable of consolidating powdered materials to produce very high densities, especially when heating is involved.

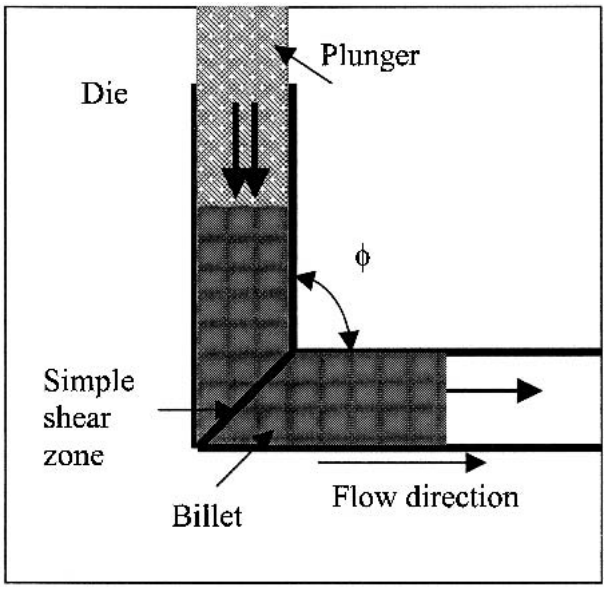

Fig. 1 Schematic diagram of the equal channel angular extrusion process

ECAE has demonstrated an impressive capability for improving the cryogenic and ambient mechanical properties and the superplastic behavior of cast alloys. Room temperature ex-

H.G. Salem, Department of Mechanical Engineering, American University in Cairo, P.O. Box. 2511 Cairo 11511, Egypt; and **J.S. Lyons,** Department of Mechanical Engineering, University of South Carolina, Columbia, SC 29208. Contact e-mail: lyons@engr.sc.edu.

periments have shown significant increase in ultimate tensile strength and ductility in the various temper conditions for the ECAE-processed alloys over the conventionally processed ones.[8] Various investigations have been conducted to study the effect of ECAE processing on the superplastic behavior and ambient temperature mechanical properties of Al-Cu-Li, Al-Mg, Al-Cu-Mg, Al-Cu-Mn, and Al-Mg-Mn-Fe base alloys.[8-12] In the current research, the effect of ECAE processing on the developed microstructure and on the superplastic behavior of an Al-Li-Cu base alloy with Zr-content less than 0.1% was investigated.

2. Experimental Procedures

2.1 Processing

The alloy used in the current research was received from the Center De Recherches De Voreppe S.A., France in the form of hot-rolled plates 17.5 mm thick with a nominal composition of Al-2.2% Li, 1.3% Cu, 0.73% Mg, and 0.05% Zr. Billets with a 296 mm^2 square cross section and a length of 152 mm were cut from the as-received plates. The billets were heat-treated to the T6 condition by solutionizing at 520 °C for 70 min and artificially aged at 190 °C for 16 h.

The ECAE process included two channels of equal cross-sectional area that intersected at an angle of $\pi/2$. In one pass through the ECAE dies, the billets were subjected to intensive shear deformation corresponding to an effective strain of 1.16.[13] The ECAE operation was repeated several times since there was no dimensional change encountered by the material after each pass. The extruded billets were fed into the channel so that the billet orientation was unchanged at each pass. Billets were brought to the extrusion temperature by placing them in a furnace for 40 min, followed by ECAE processing through the two intersecting channels heated to the same temperature to ensure controlled deforming conditions.

During ECAE processing, it is desirable to subject the material to high levels of strains at the lowest temperature possible. However, room-temperature extrusions resulted in shear localization failure after two passes. It was empirically determined that for peak-aged billets, shear localization should be avoided by a process that included four passes at 350 °C followed by four passes at 200 °C, with each pass performed at a 0.5 cm/s extrusion rate. With this multi-step process, a total effective strain of 9.36 was achieved.

2.2 Characterization

Optical and transmission electron microscopes were employed to investigate the microstructural evolution throughout the various stages of deformation via ECAE. The as-received plates' grain size was determined by light optical microscopy. Transmission electron microscopy (TEM) was used to determine subcell, subgrain, and grain sizes for the ECAE-processed billets. TEM samples were extracted from the billets after different steps in the multi-step ECAE process. A double-jet electro-polishing technique was employed for the final thinning of the TEM discs. Final thinning was performed with an electrolyte of 25% nitric acid and 75% methanol mixture at an operating voltage of 12 V, an operating current between 0.275 and 0.3 A, and at an operating temperature of −15 °C. A Phillips transmission electron microscope at 200 KV was used for the TEM examinations. Selected-area electron diffraction patterns for samples prepared from billets processed at different stages of ECAE facilitated the determination of the submicron grain sizes and grain misorientation angles. This was conducted through the determination of the zone axis from the diffraction patterns of a minimum of five touching grains in three different samples per deforming stage. Angles of misorientation were determined based on the work conducted by W. Edington.[14] Microstructural features, such as dislocation cells, subgrains, and grain sizes, were determined using an image analysis program for measuring area, length, and perimeter of subcells, subgrains, or grains in defined regions with high accuracy.

The effect of ECAE processing on the mechanical properties of the investigated alloy was conducted by measuring the hardness of the alloy after each pass at 350 and 200 °C. Hardness measurements (VHN) were conducted using a Vickers hardness tester with a 100 g load and 30 s dwell time.

The superplastic forming (SPF) behavior of the alloy was characterized with constant strain rate uniaxial tensile tests. Tensile specimens were machined parallel to the flow direction of the extruded billets after the eight-step ECAE process. The specimens had a gage length of 6.3 mm, a gage width of 0.5 mm, and a thickness of 1.6 mm. The SPF tests were conducted in a three-zone resistance heated furnace with a servohydraulic universal testing machine. Computer control of the test machine allowed the SPF tests to be performed under constant true strain rates conditions. To optimize the SPF conditions, a number of tests were performed at temperatures and strain rates ranging between 500 and 530 °C and between 2×10^{-4} and $2 \times 10^{-3} s^{-1}$, respectively.

During SPF testing, the samples were held at the test temperature for approximately 25 min prior to deformation to ensure thermal equilibrium. To understand the effect of the SPF temperature on the stability of the microstructure, additional samples of ECAE-processed material were statically annealed at the SPF temperatures for 10, 20, and 30 min. The statically annealed microstructure was examined through the transmission electron microscopy procedures previously described.

3. Results

3.1 Microstructure

Microstructural evolution was studied at different steps of the multi-step ECAE process. The as-received hot-rolled plates had a deformed structure with elongated grains parallel to the direction of rolling with variable length of several millimeters and an average width of 67 μm, as shown in Fig. 2(a). Solution heat treatment at 520 °C for 1 h followed by artificial aging at 190 °C for 16 h resulted in coarsening in the as-rolled structure from 67-92 μm in average width of the grains and with a negligible change in the length. Figure 2(b) shows an optical photomicrograph of the ECAE billets processed after four passes at 350 °C followed by four passes at 200 °C. An elongated grain structure in the direction of material flow with ultrafine substructure and coarse second-phase particles can be observed.

The microstructure of the ECAE-processed billets at the

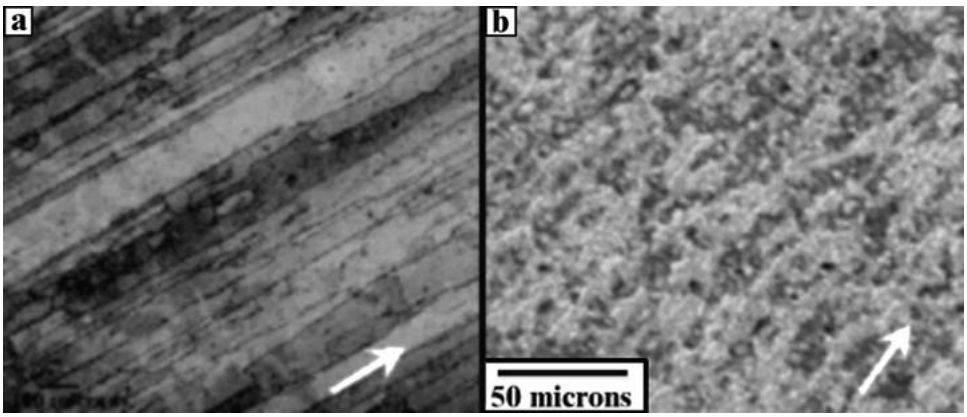

Fig. 2 Optical photomicrographs for 2098 **(a)** as-rolled and **(b)** after ECAE processing for four passes at 350 °C plus four passes at 200 °C with a cumulative effective strain of 9.3 mm/mm. Arrows indicate the direction of material flow for the rolled as-received plates and the ECAE billets.

different stages of extrusion was investigated using TEM. Figure 3(a) shows a TEM bright-field micrograph of the billets processed after one pass at 350 °C, where a high density of tangled dislocations was generated within the hot-rolled grains and along their boundaries. Moreover, dislocation bands were observed within the structure (Fig. 3a, marked by arrows). Increasing the applied strain from 1.16 up to 4.6 by extruding the billets through four passes at 350 °C resulted in the formation of a heterogeneous substructure within the as received grains. Figure 3(b) shows an inhomogeneous degree of dynamic recovery that was manifested in the formation of ultrafine dislocation cells (marked A) and 0.5 μm subgrains that were dislocation free at the interior (marked B) but had high dislocation density at the boundaries. An obvious coarsening of the second-phase particles was revealed, as shown in Figure 3(b) (marked C), which is attributed to over-aging at elevated extrusion temperatures. The formed subgrain's misorientation was $\leq 2°$ for most of the fragmented as-received grains.

Billets processed for four passes at 350 °C followed by one pass at 200 °C had a cumulative effective strain of $\epsilon_{eff} = 5.8$ mm/mm. Examination of the material in this condition revealed the formation of a completely different microstructure as compared to the recovered one at 350 °C. A heterogeneous microstructure was formed, which consisted of areas of both equiaxed and elongated substructure with many nonequilibrium boundaries. Figure 4(a) shows a TEM micrograph at a relatively low magnification for a billet processed for four passes at 350 °C and one pass at 200 °C. Due to the limited dynamic recovery at a low deformation temperatures, a structure with undefined boundaries about 0.5 μm in size was formed. Figure 4(b) shows a higher magnification micrograph for the region indicated by the arrow on Figure 4(a). Subcells about 0.1-0.2 μm in size were developed by additional fragmentation of the 0.5 μm recovered structure developed at earlier extrusion passes at 350 °C. Although some boundaries had high dislocation density, other sides revealed the formation of wider boundaries associated with dislocations, which indicates an advanced stage of dynamic recovery.

Figure 5 shows TEM micrographs for billets after the fourth pass at 200 °C with a total accumulation of eight passes and a total effective strain of 9.3 mm/mm. Figure 5(a) shows regions with fragmented submicron grains about 0.4 μm in average size, similar to those observed in the processed billets for four passes at 350 °C with one pass at 200 °C (Fig. 4b). Other regions shown in Fig. 5(b) revealed the evolution of well-defined, equiaxed, highly misoriented substructure about 0.4 μm in average size, which constituted most of the developed structure.

Figure 6 shows a misorientation angle histogram for the billets processed for four passes at 350 °C with one pass at 200 °C versus that for billets processed for four passes at 350 °C with four passes at 200 °C. Almost 70% of the developed structure had low-angle boundaries, ranging from 3.5-8° for the five-pass billets. A very small fraction of subgrains displayed high-angle misorientation greater than 15°. However, intense plastic straining accumulated at the end of eight passes resulted in the increase in misorientation angles between the formed subgrains. In the eight-pass material, about 55% of the developed submicron grain structure had measured misorientation angles ranging between 7-14°.

3.2 Hardness

Vickers hardness measurements after each step of the ECAE process provided additional information about the microstructural development and mechanical behavior. Figure 7 shows the Vickers hardness variation with the cumulative true effective strain for the processed billet after each of the four passes at 350 °C and four passes at 200 °C. Severe softening took place during the first and second passes at 350 °C. A slight and gradual decrease was observed with increasing the number of passes from two-four with a cumulative total effective strain of 4.64 mm/mm. An obvious increase in hardness was exhibited by the billets ECAE processed with one pass at 200 °C, where about 53% of the lost hardness was restored. A slight and gradual decrease in hardness values took place with an increase in the cumulative effective true strain from 5.8 (5 passes) to 9.3 mm/mm (8 passes).

3.3 Superplastic Behavior

Uniaxial tension superplastic tests were conducted using the 2098 material after it had completed the eight-step ECAE process. The results are shown in Fig. 8. The test conducted at 500

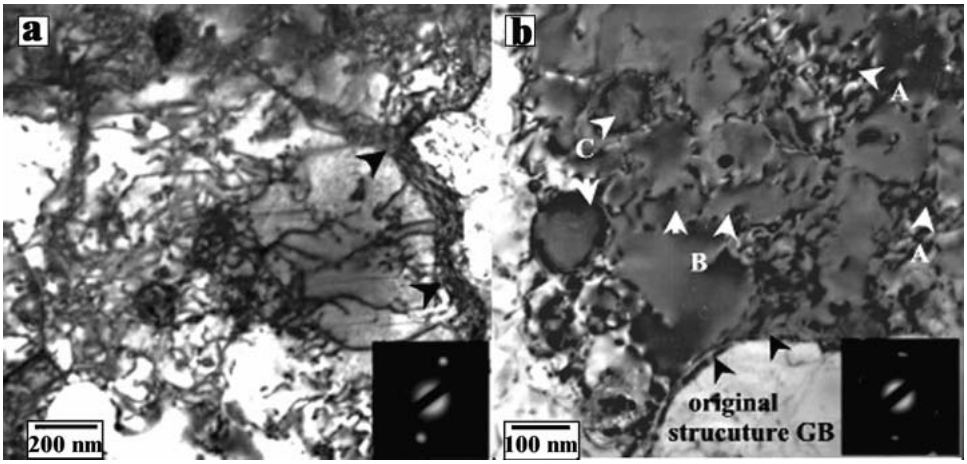

Fig. 3 TEM bright-field micrographs for **(a)** ECAE processed billets for one pass at 350 °C (ϵ_{eff} = 1.16 mm/mm) with a SADP parallel to the $[112]_{Al}$ zone axis and **(b)** the ECAE processed billets four passes at 350 °C (ϵ_{eff} = 4.64 mm/mm) with a SADP parallel to the $[011]_{Al}$ zone axis

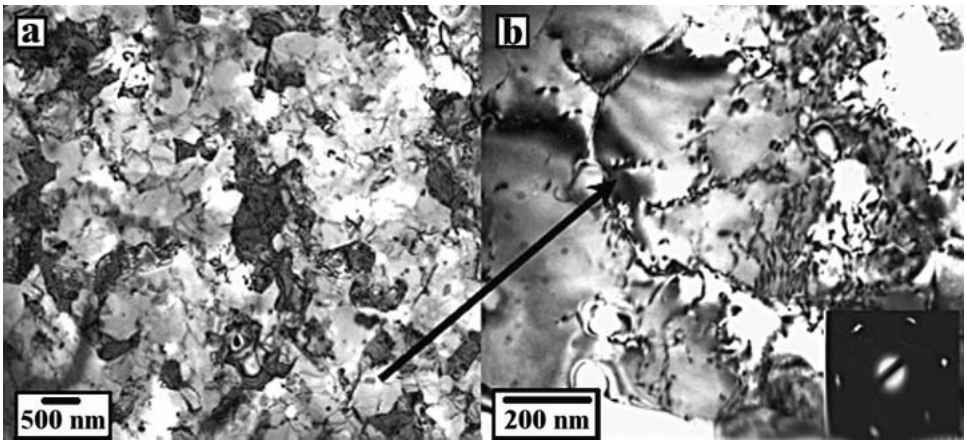

Fig. 4 TEM bright-field micrographs for ECAE processed billets for four passes at 350 °C plus one pass at 200 °C (ϵ_{eff} = 5.8 mm/mm) at **(a)** low magnification and **(b)** high magnification with a SADP parallel to the $[111]_{Al}$ zone axis

°C and 2×10^{-3} s^{-1} had a peak flow stress of about 15 MPa that remained nearly constant between true strains of 0.6 and 0.9. The elongation-to-fracture for this test was 270% (true strain ~ 1.2). Raising the temperature to 530 °C at the same strain rate resulted in a lower flow stress and greater elongation. The flow stress of the 530 °C, 2×10^{-3} s^{-1} test was about 12 MPa and remained relatively constant between true strains of 0.6 and 1.2, and the elongation-to-fracture was about 330% (true strain ~ 1.5). Lowering the strain rate to $2 \times 10^{-4} s^{-1}$ and keeping the test temperature at 530 °C resulted in a further reduction in flow stress, to about 10 MPa. However, the elongation-to-fracture was reduced to just 125% (true strain ~ 0.8). Of the test conditions investigated, the processing conditions of 530 °C and 2×10^{-3} s^{-1} appear to be optimum. In all cases, however, the flow stress decreased from its peak value near the end of the test. This is attributed to cavitation, as discussed in the next section.

In an attempt to understand why the elongation-to-fracture decreased with decreased strain rate at 530 °C, samples were extracted from the eight-pass billet and statically annealed at 530 °C for 10, 20, and 30 min. TEM was used to examine the structure in these samples as a function of annealing time. As shown in Fig. 9, static annealing of the dynamically recovered structure produced by ECAE processing caused grain growth. For example, after 10 min of static annealing at 530 °C, the grain size increased to about 2 μm, with dislocations within the grains in the form of dislocation helices and Orowan loops surrounding $\delta'(Al_3Li)$ coherent precipitates. Moreover, extinction contours with dislocations were observed along the coarsened grains boundaries. Figure 9(b) shows the grain structure after 20 min of static annealing at 530 °C, in which grain growth up to 5 μm in average size was observed. An unstable grain growth was observed for the billets annealed for 30 min, where the measured grain size ranged between 9-12 μm. In addition, clustering of the $\beta'(Al_3Zr)$ precipitate was observed within the coarsened grains as shown in Fig. 9(c). Evolution of a relaxed structure with high angle grain boundaries is manifested by the formation of smooth, sharp, well-defined, hexagon-shaped boundaries. It is postulated that grain growth during heat-up and testing is in part responsible for the relatively poor superplastic behavior of the 530 °C, 2×10^{-4} s^{-1} test specimen.

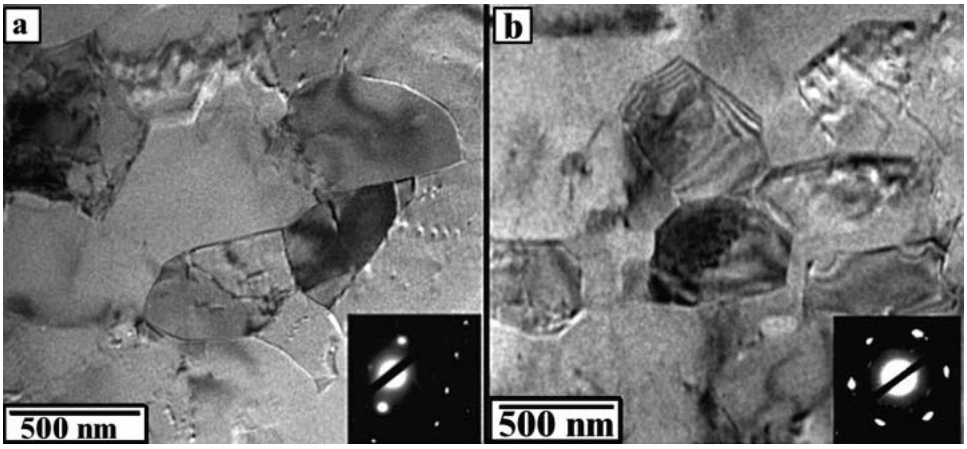

Fig. 5 TEM bright-field micrographs after ECAE processing for four passes at 350 °C plus four passes at 200 °C with a SADP parallel to the $[112]_{Al}$ zone axis**. (a)** A fragmented structure with small misorientations, and **(b)** equiaxed, well-defined, highly misoriented subgrain structure with a SADP parallel to $[\bar{1}11]_{Al}$ zone axis

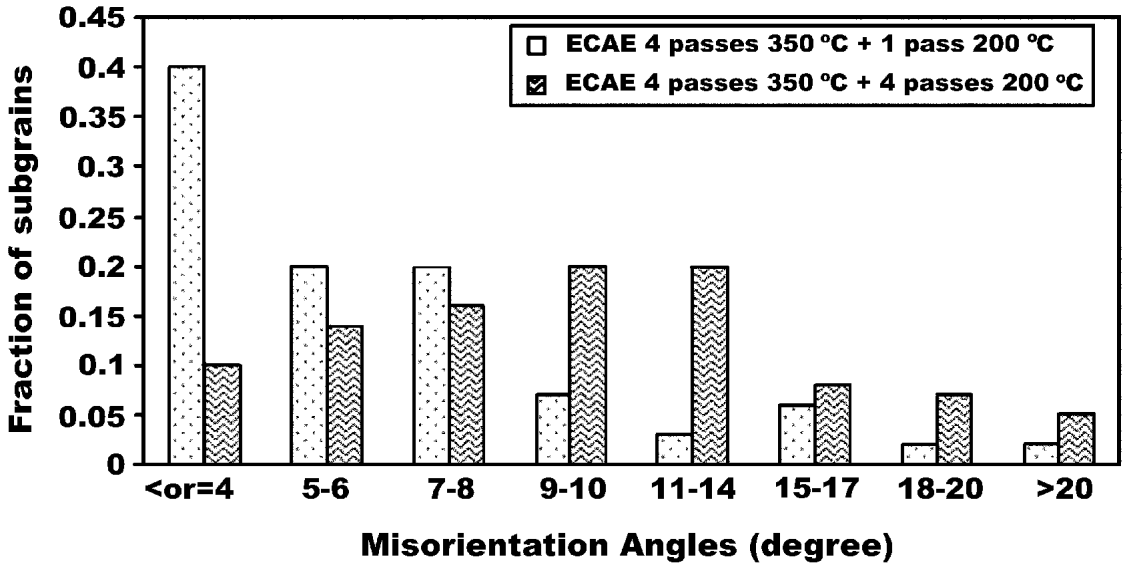

Fig. 6 Misorientation angle histogram for billets ECAE processed for four passes at 350 °C plus one pass at 200 °C (ϵ_{eff} = 5.8 mm/mm) and four passes at 350 °C plus four passes at 200 °C (ϵ_{eff} = 9.3 mm/mm)

4. Discussion

Results of the current research proved that ECAE process is capable of grain refinement to the submicron level when conducted not only on a direct chill slabs,[8, 9] but also on hot-rolled plates with finer grain structures. At early stages of straining (ϵ_f = 1.16) at 350 °C, a high dislocation density is generated at the grain and particle boundaries of the hot rolled structure, especially around the coarsened second-phase particles. Preheating and deformation at 350 °C results in second-phase particle overaging and hence softening of the matrix, which explains the significant decrease in VHN-values (Fig. 7), which facilitates successive deformation at lower temperatures (200 °C).

Increasing the number of passes at 350 °C led to the development of a fragmented structure in the form of dislocation cells with very small angles of misorientation. This result agrees with the findings of Sinclair et al.[15] They concluded that Al alloys should be deformed by intense plastic straining at warm temperatures ≤ 300 °C to allow for the development of dynamically recovered high-angle grain boundaries that is necessary for successive deformation for optimum superplasticity.

The 2098 billets processed by ECAE likely developed subgrains by dynamic recovery. This is different from the Al-Cu-Li alloys 2095 and 2195 processed under similar conditions,[16] which exhibit evidence of particle-stimulated nucleation.[17, 18] At the processing temperature of 350 °C, 2095 and 2195 fall in the Al_{ss} + T_B (Al_7CuLi) + T_1 (Al_2CuLi) and Al_{ss} + T_B phase regions, respectively, where A_{ss} represent the phases in solid

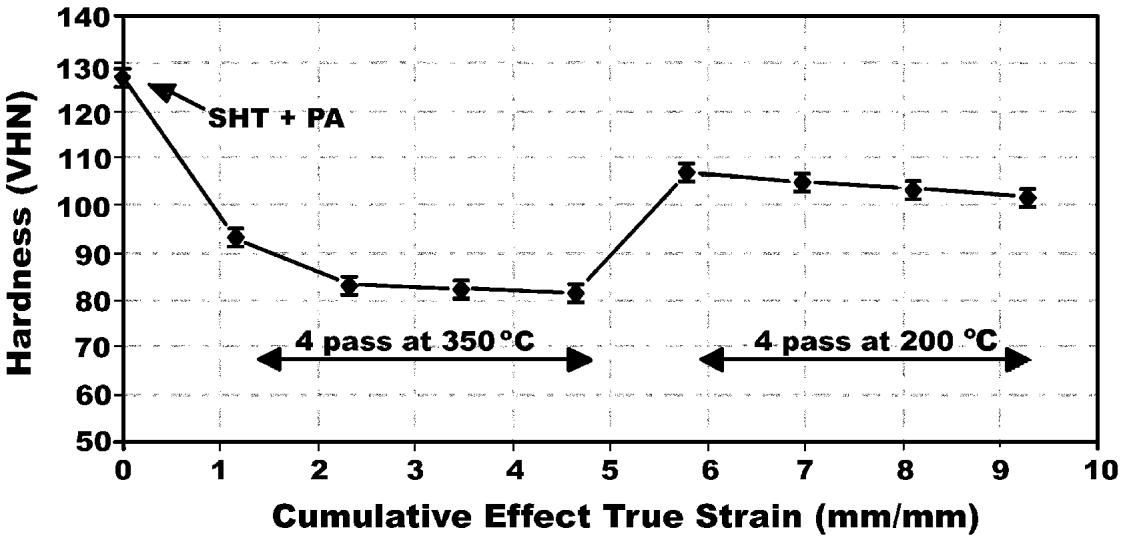

Fig. 7 Hardness variation as a function of the number of ECAE passes. The first four passes were at 350 °C; the next four passes were at 200 °C. The effective strain per pass was 1.16, giving a total cumulative effective strain of 9.3 mm/mm.

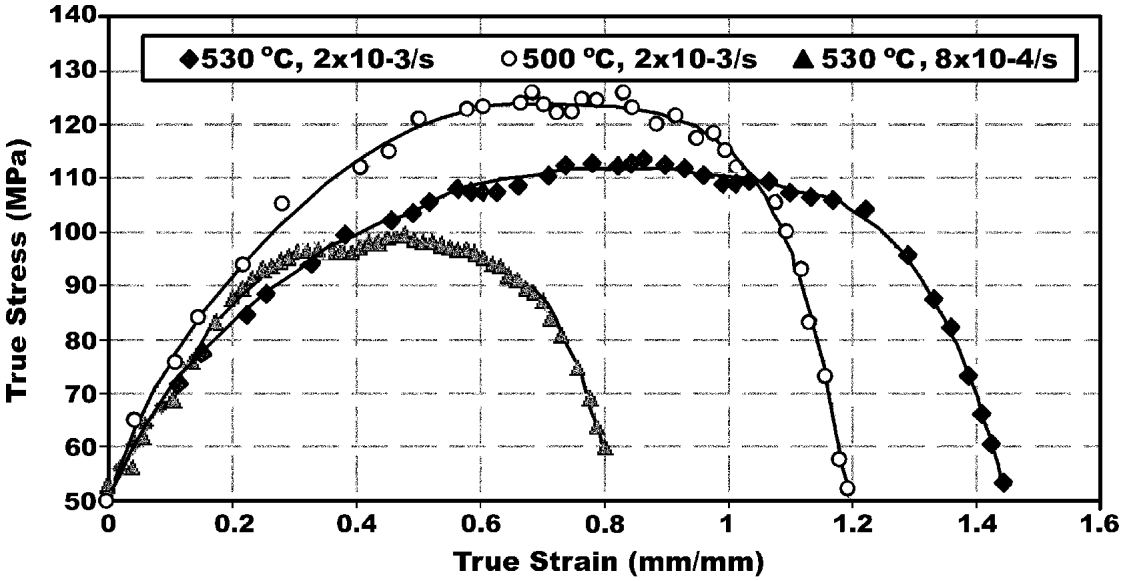

Fig. 8 Superplastic uniaxial tension test results (true stress-strain diagram) for 2098 after ECAE processing for four passes at 350 °C plus four passes at 200 °C with cumulative effective strain of 9.3 mm/mm

solution.[16,19] This is due in part to their Cu:Li ratio being greater than 4. On the other hand, the 2098 Al-Li-Cu alloy system has a Cu:Li ratio < 1, and at 350 °C falls in the Al_{ss} + T_2 + + δ (AlLi) phase region. Thus in the current work, the low volume fraction and small size (≤ 100 nm) of the particles within the matrix of 2098 alloy do not effectively promote a finer, well-defined structure by particle-stimulated nucleation.[20, 21]

ECAE processing for a single pass at 200 °C results in an increase in the dislocation density and severe fragmentation of the substructure, which enables the formation of subcells and hence restoration of most of the lost hardness exhibited by the first four passes at 350 °C. The observed slight decrease in VHN-values from 107-102 after the sixth, seventh, and eighth passes could be due to the dynamic recovery that takes place at warm deforming temperatures. A total accumulation of eight passes corresponding to a total effective strain of 9.3 mm/mm develops a well-defined submicron grain structure with high misorientation angles ranging between 9° and 14°, which agrees with the findings of Bowen et al.[22]

Optimum superplastic properties for 2098 alloy after ECAE processing via four passes at 350 °C with four passes at 200 °C were found to be at a superplastic forming temperature of 530°C and strain rate of $2 \times 10^{-3} s^{-1}$. It should be noted that the optimum strain rate for the ECAE processed alloy is an order of magnitude lower than that exhibited by 2098 when it is

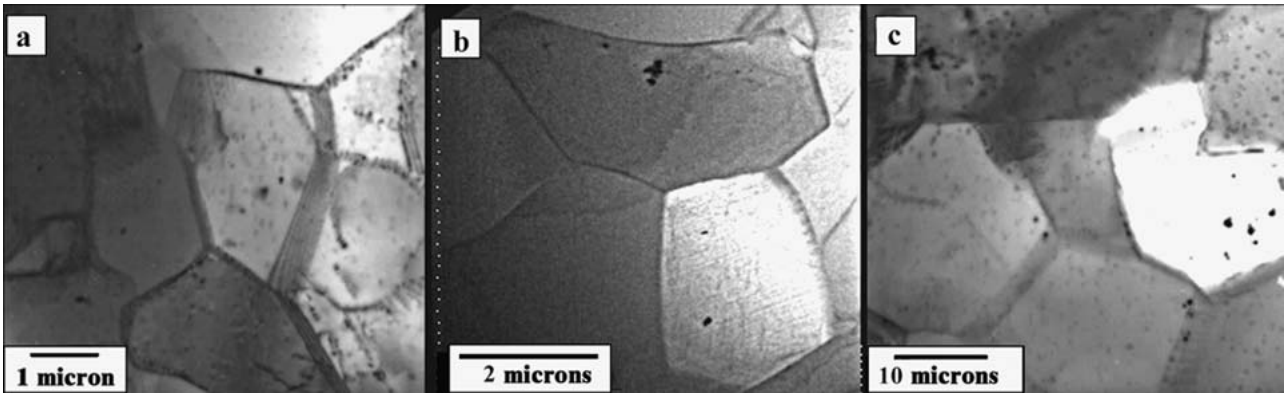

Fig. 9 TEM bright-field micrographs for four passes at 350 °C plus four passes at 200 °C, ECAE processed 2098 after static annealing at 530 °C for **(a)** 10 min, **(b)** 20 min, and **(c)** 30 min

conventionally processed via rolling.[23] Work done on 2098 superplastic sheets processed by rolling indicated that a maximum of 140% elongation-to-fracture is encountered at deforming temperatures of 480 °C, and strain rates of $10^{-4}s^{-1}$, and are even worse at higher deforming temperatures.[23] Therefore, ECAE processing is capable of improving the superplastic behavior of the 2098 alloy significantly, regardless of the low volume fraction of β′ phase, and hence creating better cost effectiveness.

The observed flow stress decrease with increasing strain (Fig. 8) could be a result of either significant grain growth associated with the SPF temperature or an unaccomodated grain boundary sliding that enhances cavities nucleation and growth followed by premature fracture. Quing et al.,[24] who worked with superplastic Al-Li-Cu base alloys, and Matsuo,[25] who worked with a superplastic 5083 alloy, observed similar behavior. The observed submicron grain coarsening of the ECAE processed billets from 0.5-10 μm (Fig. 9) during static annealing experiments supports this hypothesis. Conversely, Al alloys investigated earlier by Furukawa et al. [6] and Salem et al.[16] remained reasonably constant with an average size of < 2 μm at similar annealing temperatures. The primary factor that enabled grain growth is the low volume fraction of the β′ phase (0.05% Zr) and its clustering at elevated temperatures (Fig. 9c), which is microstructurally different from alloys with Zr-content > 0.12 %.[6, 16] Moreover, the high energy contained in the heavily strained microstructure prior to subsequent static or dynamic heating results in rapid grain growth and hence cavitation, which is a typical problem encountered by Al alloys during superplastic formation.[24-28] The lack of grain growth inhibitors results in a relatively low elongation-to-fracture (premature fracture) at the elevated temperatures associated with superplastic forming. Accordingly, to preserve the submicron grain structure developed by ECAE that enables large amounts of Superplasticity, the presence of high volume fraction of fine, coherent, and uniformly distributed precipitate stable against dissolution at elevated temperatures is necessary to hinder grain growth.

5. Conclusions

ECAE processing develops a submicron grain structure with size and shape that depend on the deforming temperature and the total effective strain. Extruding 2098 billets without changing their orientation between passes develops submicron structure < 0.5 μm in average size. Hot working at temperatures > 0.5 T_m is necessary to establish a dynamically recovered substructure and coarsened second-phase particles. This softens the material for subsequent processing at lower temperatures. Warm working at temperatures ≤ 0.4 T_m results in refinement of the developed structure and an increase in the misorientation angles with an increase in the number of passes.

The capability of ECAE processing for improving the overall superplastic elongation-to-fracture by 235% for 2098 has been proved. Optimum superplasticity for the ECAE-processed 2098 alloy is achieved at strain rates of an order of magnitude higher than that of the conventionally processed 2098. However, the effectiveness of grain refinement to the submicron grain size during the elevated temperature superplastic forming is affected by the low volume fraction of fine, coherent, and uniformly distributed grain-growth inhibitors.

Acknowledgments

The authors thank the Center De Recherches De Voreppe S.A., France, for donating the material investigated in the current research, and the Department of Mechanical Engineering, Texas A&M University for processing of the alloy by ECAE. The support of the U.S.-Egypt Science and Technology Program and the National Science Foundation Division of International Programs (Award 0108894) is gratefully acknowledged.

References

1. W. Kim, E. Taleff, and O.D. Sherby: *Scripta Metall*., 1995, *32,* pp. 1625-32.
2. A. Ghosh and C. Gandhi: "Characterization of Superplastic Behavior in an Aluminum Lithium Alloy" in *ICSMA-7*, H. McQueen et al., ed., Pergamon Press, Oxford, 1986, p. 2065
3. M. Mamuro and K. Higashi: *JOM*, 1998, *50*(6), pp. 34-39.
4. Y. Iwahashi, J. Wang, Z. Horita, N. Nemoto, and T. Langdon: *Scripta Metall*., 1996, *35*(2), pp. 143-46.
5. Y. Iwahashi, M. Furukawa, Z. Horita, M. Nemoto, and T. Langdon: *Metall. Mater. Trans. A*, 1998, *29A,* pp. 2245-52.
6. M. Furukawa, et al., *Mater. Sci. Forum*, 1999, *233-34,* pp. 177-84.
7. J. Pickens, F. Heubaum, J. Langan, and L. Kramer: "Aluminum Lithium 5," *Conference Proceedings*, T. Sanders and E. Strake Jr., ed.,

Materials and Component Engineering, Birmingham, United Kingdom, 1989, pp. 1397-414.
8. H.G. Salem and R. Goforth: "Influence of Intense Plastic Straining on Room Temperature Mechanical Properties of Al-Cu-Li Base Alloys," *Cairo University International Conference MDP7,* Feb. 15-17, 2000, pp. 357-68.
9. H.G. Salem, R.E. Goforth, and K.T. Hartwig: "Superplastic Characterization of 2095 Al-Li Alloys Processed by Equal Channel Angular Extrusion," *Superplasticity and Superplastic Forming, Proc. TMS,* A. K. Ghosh et al., ed., 1998, pp. 165-96.
10. J. Wang, Z. Morita, M. Furukawa, K. Kolai, R. Valiev, M. Yan, and T. Langdon: *J. Mater. Res.,* 1993, *8*(11), pp. 2810-18.
11. Z. Horita, T. Fujinami, M. Nemoeo, and T. Langdon: *Metall. Mater. Trans. A*, 2000, *31A,* pp. 691-701.
12. L. Yong and T.G. Langdon: *J. Mater. Sci.,* 2000, *35*(5), pp.1201-04.
13. V. Segal, "Working of Metals by Simple Shear Deformation Process," *Proc. 5th International Aluminum Extrusion Technology Seminar,* 1992, *2,* p. 403.
14. J.W. Edington: *Practical Electron Microscopy in Materials Science*, New York, NY, 1976.
15. J. Sinclair: "Microstructure And Mechanical Properties of Aluminum 5083 Processed by Equal Channel Angular Extrusion," Ph.D. Dissertation, Texas A&M University, College Station, TX, 1999.
16. H.G. Salem: "Influence of Equal Channel Angular Extrusion Processing on the Physical, Mechanical, and Microstructural Properties of Al-Cu-Li Base Alloys," Ph.D. Dissertation, Texas A&M University, College Station, TX, 1997.
17. C. Zener and C. S. Smith: *Trans. Metall. Soc*., AIME, Cleveland, 1984, p. 54.
18. R. Sandström: in *The First Riso Symposium on Metallurgy and Materials Science*, N. Hansen and T. Lefters, ed., Risø National Laboratory, Roskilde, Denmark, 1980, p. 45.
19. J. M. Silcock: *J. Inst. Meth,* 1988, *1959-60,* p. 357.
20. J. Wadwarth, A. Petton, and R. Lewis: *Metall. Tran A*, 1985, *16A,* pp. 2319-32.
21. E. Lavernia, T. Srivatsan, and F. Mohamed: *J. Mater. Sci.*, 1990, *25,* pp. 1137-158.
22. J.R. Bowen, P.B. Prangnell, and F.J. Humphreys: *Mater. Sci. Technol.,* 2000, *16,* pp. 1246-51.
23. B. Iskander: "Effect of Thermomechanical Treatments on The Ductility of Al-Li Alloy," Ph.D. Dissertation, Metallurgical Engineering, Cairo University, Cairo, Egypt, 1995.
24. L. Quing, Y. Jinfing, and Y. Mel: *Scripta Metall.,* 1991, *25,* 109-14.
25. M. Matsuo: "Properties of Superplastic 5083 Alloy and its Applications" in S*uperplasticity and Superplastic Forming,* A. Ghosh and T. R. Bieler, ed., The Minerals, Metals & Materials Society, Denmark, 1995, pp. 277-83.
26. J. Pilling and N. Ridley: *Superplasticity in Crystalline Solids,* Institute of Metals, London, United Kingdom, 1988.
27. F. Humphreys and M. Hatherly: *Recrystallization and Related Annealing Phenomena,* Elsevier Science Ltd., Tarrytown, NY, 1996, p. 167.
28. M. Zaidi and J. Wert: *Treatise on Materials Science and Technology*, G. Mahon and R. Ricks, ed., USA, 1989, p. 139.